Latin American Journal of Solids and Structures
www.lajss.org

Three dimensional vibration and bending analysis of carbon nano-tubes embedded in elastic medium based on theory of elasticity

Abstract

This paper studies free vibration and bending behavior of single-walled carbon nanotubes (SWCNTs) embedded on elastic medium based on three-dimensional theory of elasticity. To accounting the size effect of carbon nanotubes, non-local theory is adopted to shell model. The nonlocal parameter is incorporated into all constitutive equations in three dimensions. The surrounding medium is modeled as two-parameter elastic foundation. By using Fourier series expansion in axial and circumferential direction, the set of coupled governing equations are reduced to the ordinary differential equations in thickness direction. Then, the state-space method as an efficient and accurate method is used to solve the resulting equations analytically. Comprehensive parametric studies are carried out to show the influences of the nonlocal parameter, radial and shear elastic stiffness, thickness-to-radius ratio and radius-to-length ratio.

Keywords

carbon nano-tubes; embedded; nonlocal; 3D elasticity; free vibration; bending

M. Shaban [a]
A. Alibeigloo [b]

[a] Department of Mechanical Engineering, Tarbiat Modares University, Tehran, Iran.
m.shaban@modares.ac.ir

[b] Department of Mechanical Engineering, Tarbiat Modares University, Tehran, Iran. abeigloo@modares.ac.ir, corresponding author.

Received 15.05.2014
In revised form 29.06.2014
Accepted 18.08.2014
Available online 26.09.2014

1 INTRODUCTION

In the last two decades, carbon nano-tubes (CNTs) have attracted the attention of many research groups due to its exceptional mechanical, chemical and electrical properties. The mechanical characteristics of CNTs is of great interest for engineering design and manufacture especially in nano-electro-mechanical systems (NEMS) and numerous techniques for modeling the CNTs has been carried out along with experimental researches. Since experimental investigations are expensive at nano-scale systems, theoretical modeling of CNTs has received increasing attention in recent years.

There are several works studies the mechanical behavior of CNTs by using classical theories. He *et al.* (2005) presented an explicit definition of the vdWs coefficient and studied the axial buckling of CNTs. Hu *et al.* (2007) and Hu *et al.* (2008) utilize string-elastic shell model for studying the

vibration and buckling forces of a carbon nanowire. An excellent survey of the research work on the classical model of CNTs can be found in the work done by Gibson *et al.* (2007). Recently, Ansari and his co-workers (Ansari, Hemmatnezhad, *et al.* (2011), Ansari and Sahmani (2011)) used various beam models to study the vibration and buckling of single-walled carbon nano-tubes (SWCNTs).

However, both experimental and atomistic simulations have shown that nanostructures have size-dependent behavior so that well-known classical theories cannot capture this behavior of nanostructures. It means when the size of the structure becomes small, as well as the nanostructure, the small length effect (such as lattice spacing between individual atoms) becomes gradually more important and thus its effects can no longer be ignored (Sun and Zhang (2003), Aydogdu (2012)) . Nonlocal theory is one of the well known continuum models that includes internal length scale and has good accuracy compared with experimental results (Eringen (2002)). This theory includes length scale effect and long-range atomic interactions so that it can be considered as a continuum model for atomic lattice dynamics. Many researchers incorporated nonlocal theory into beam model to study vibration, bending and buckling of CNTs. Wang *et al.* (2006) utilized Timoshenko beam theory to analyzed buckling of nano tubes based on nonlocal elasticity. They compared nonlocal results with classical beam theories and showed that small scale effect reduces the critical buckling load. Reddy (2007) studied bending, vibration and buckling of nanobeams and reformulated various beam theories by using the nonlocal theory. Wang and Liew (2007) studied bending behavior of SWCNs by using nonlocal Euler–Bernoulli and Timoshenko beam theory. Based on nonlocal theory, Thai (2012) used shear deformation beam theory to study deflection, buckling and natural frequency of nano-beam. He presents analytical solution for simply supported beam by implementing series expansion. Eltaher *et al.* (2012) studied free vibration behavior of functionally graded (FG) nanobeams by using Euler–Bernoulli beam theory. In their work, the size-dependent behavior is considered by utilizing nonlocal constitutive relation. Shen *et al.* (2012) modeled CNT-based biosensor by using nonlocal Timoshenko beam theory. They assumed that multiwall CNT carrying a spherical nanoscale bio- object at the free end and used transfer function method to determine the natural frequencies of CNTs. On the basis of nonlocal theory, Aydogdu and Filiz (2011) used classical beam model to study the small-scale effect on axial vibration behavior of SWCNTs. They showed that the axial vibration frequencies of SWCNT with attached mass are highly overestimated by using the classical beam theory. Based on nonlocal theory, Murmu *et al.* (2011) used nonlocal beam model to study the torsional vibration behavior of SWCNTs with added buckyballs at one end.

There are several studies, in which the mechanical behaviors of CNTs are investigated by using nonlocal shell model. Arash and Ansari (2010) used first order shear deformation shell theory to model SWCNTs. They considered that SWCNT is subjected to initial strain and solved the nonlocal equations by radial point interpolation method. Yan *et al.* (2010) investigated the small scale effect on the buckling behavior of triple-walled carbon nanotubes (TWCNTs) with nonlocal theory. They modeled TWCNTs as three elastic shells and considered axial load in thermal environment. Khademolhosseini *et al.* (2010) developed modified nonlocal continuum shell model based on nonlocal theory and studied torsional buckling of SWCNTs. They showed that classical shell models overestimate the buckling torques. Hao *et al.* (2010) used nonlocal theory to study the small-scale effect on the torsional buckling of multi-walled carbon nano-tubes (MWCNTs). They used multiple-shell model for the MWCNT surrounded by an elastic medium and subjected to the thermal load.

Ansari, *et al.* (2011) studied free vibration response of double-walled carbon nanotubes based on Rayleigh–Ritz technique. They incorporated nonlocal elasticity theory into the classical Donnell shell theory. Ansari *et al.* (2011) investigated the buckling behavior of CNTs by using nonlocal shell theory. They used Rayleigh–Ritz method in conjunction with the set of beam functions. Wang *et al.* (2012) investigated the effect of nonlocal parameters on the vibration of CNTs based on nonlocal shell and beam models. They showed that circumferential nonlocal effect is considerable in vibration of CNTs compared with existing molecular dynamics simulations. Recently, authors used three dimensional theory of elasticity to analysis the vibration behavior of nano-plate and CNTs (Alibeigloo (2011); Alibeigloo (2012); Alibeigloo and Pasha Zanoosi (2013); Alibeigloo and Shaban (2013)).

To the best of author knowledge, the three dimensional bending and vibration behavior of CNTs surrounded by polymer matrix in conjunction with nonlocal theory has not yet been investigated, and the present work attempts to consider this analysis. The surrounding matrix is assumed to have both shear and transverse flexibilities, so that the two parameters elastic foundation based on Winkler and Pasternak model is considered (Yoon (2003); Murmu and Pradhan (2009)). The partial differential equations are reduced to the ordinary equations by expanding the field variables to double Fourier series along the axial and circumferential coordinates. Due to its efficiency, the state-space technique is applied to the equations in radial direction and obtain the stress and displacement fields.

2 GOVERNING EQUATION

Here, we applied three-dimensional elasticity theory in combination with nonlocal theory to study the bending and vibration behavior of SWCNs. In the nonlocal theory, unlike the conventional local theories, it is assumed that the stress at a point in a continuum body is function of the strain at all neighbor points of the continuum. Constitutive model that expresses the nonlocal stress tensor is as follow:

$$\left(1-\mu\nabla^2\right)t_{ij}=\sigma_{ij}=c_{ijkl}\varepsilon_{kl} \tag{1}$$

where μ is the nonlocal parameter, t_{ij} is the nonlocal stress tensor, σ_{ij} is the local stress tensor, c_{ijkl} is the fourth-order elasticity tensor and ε_{ij} is the local strain tensor. Fig. 1 shows SWCN in cylindrical coordinate *(r,θ,z)* surrounded by polymer matrix. L, R_{i}, R_{o}, and h is the length, inner radius, outer radius and thickness. As shown in Fig. 1, the surrounding matrix is modeled as two-parameter elastic foundation. Governing equations of motion for SWCNs, in cylindrical coordinate are

$$\begin{cases} \dfrac{\partial\sigma_r}{\partial r}+\dfrac{1}{r}\left(\sigma_r-\sigma_\theta\right)+\dfrac{\partial\tau_{rz}}{\partial z}+\dfrac{1}{r}\dfrac{\partial\tau_{r\theta}}{\partial\theta}=\rho\dfrac{\partial^2u_r}{\partial t^2} \\ \dfrac{\partial\tau_{rz}}{\partial r}+\dfrac{1}{r}\tau_{rz}+\dfrac{\partial\sigma_z}{\partial z}+\dfrac{1}{r}\dfrac{\partial\tau_{z\theta}}{\partial\theta}=\rho\dfrac{\partial^2u_z}{\partial t^2} \\ \dfrac{\partial\tau_{r\theta}}{\partial r}+\dfrac{2}{r}\tau_{r\theta}+\dfrac{\partial\tau_{z\theta}}{\partial z}+\dfrac{1}{r}\dfrac{\partial\sigma_\theta}{\partial\theta}=\rho\dfrac{\partial^2u_\theta}{\partial t^2} \end{cases} \tag{2}$$

Based on non-local theory, the constitutive relations in three-dimensional theory of elasticity are written as

$$\begin{aligned}
\sigma_r - \mu\nabla^2\sigma_r &= C\Big[\big(1-\nu\big)\varepsilon_r + \nu\big(\varepsilon_\theta + \varepsilon_z\big)\Big] \\
\sigma_\theta - \mu\nabla^2\sigma_\theta &= C\Big[\big(1-\nu\big)\varepsilon_\theta + \nu\big(\varepsilon_r + \varepsilon_z\big)\Big] \\
\sigma_z - \mu\nabla^2\sigma_z &= C\Big[\big(1-\nu\big)\varepsilon_z + \nu\big(\varepsilon_r + \varepsilon_\theta\big)\Big] \\
\tau_{zr} - \mu\nabla^2\tau_{zr} &= C'\gamma_{zr} \\
\tau_{r\theta} - \mu\nabla^2\tau_{r\theta} &= C'\gamma_{r\theta} \\
\tau_{\theta z} - \mu\nabla^2\tau_{\theta z} &= C'\gamma_{\theta z}
\end{aligned} \tag{3}$$

where μ is the nonlocal parameter and $C = \dfrac{E}{\big(1+\nu\big)\big(1-2\nu\big)}$, $C' = \dfrac{E}{2\big(1+\nu\big)}$.

$\nabla^2 = \dfrac{\partial^2}{\partial r^2} + \dfrac{1}{r}\dfrac{\partial}{\partial r} + \dfrac{1}{r^2}\dfrac{\partial^2}{\partial\theta^2} + \dfrac{\partial^2}{\partial z^2}$ is the 3D Laplacian operator. The linear relations between the strain and the displacement are express

$$\begin{aligned}
\varepsilon_r &= \frac{\partial u_r}{\partial r} & \gamma_{r\theta} &= \frac{1}{r}\frac{\partial u_r}{\partial\theta} + \frac{\partial u_\theta}{\partial r} - \frac{u_\theta}{r} \\
\varepsilon_\theta &= \frac{1}{r}\frac{\partial u_\theta}{\partial\theta} + \frac{u_r}{r} & \gamma_{z\theta} &= \frac{\partial u_\theta}{\partial z} + \frac{1}{r}\frac{\partial u_z}{\partial\theta} \\
\varepsilon_z &= \frac{\partial u_z}{\partial z} & \gamma_{rz} &= \frac{\partial u_r}{\partial z} + \frac{\partial u_z}{\partial r}
\end{aligned} \tag{4}$$

The stress-displacement relations for the SWCN by using Eqs. (3) and (4) can be written as

$$\sigma_r - \mu\nabla^2\sigma_r = C\left[\big(1-\nu\big)u_{r,r} + \frac{\nu}{r}\big(u_{\theta,\theta} + u_r\big) + \nu u_{z,z}\right] \tag{5-1}$$

$$\sigma_\theta - \mu\nabla^2\sigma_\theta = C\left[\nu\, u_{r,r} + \frac{1-\nu}{r}\big(u_{\theta,\theta} + u_r\big) + \nu u_{z,z}\right] \tag{5-2}$$

$$\sigma_z - \mu\nabla^2\sigma_z = C\left[\nu\, u_{r,r} + \frac{\nu}{r}\big(u_{\theta,\theta} + u_r\big) + \big(1-\nu\big)u_{z,z}\right] \tag{5-3}$$

$$\tau_{rz} - \mu\nabla^2\tau_{rz} = C'\big(u_{z,r} + u_{r,z}\big) \tag{5-4}$$

$$\tau_{r\theta} - \mu\nabla^2\tau_{r\theta} = C'\left(\frac{1}{r}u_{r,\theta} + u_{\theta,r} - \frac{u_\theta}{r}\right) \tag{5-5}$$

$$\tau_{z\theta} - \mu\nabla^2\tau_{z\theta} = C'\left(u_{\theta,z} + \frac{1}{r}u_{z,\theta}\right) \tag{5-6}$$

The equations of motion in term of displacement components can be written as below Alibeigloo and Shaban (2013)

$$\begin{aligned} &C\left(1-\nu\right)u_{r,rr}+\frac{C}{r}\left(1-\nu\right)u_{r,r}-\frac{C}{r^2}\left(1-\nu\right)u_r+\frac{C'}{r^2}u_{r,\theta\theta}+\frac{C}{2}u_{z,zr}\\ &+C'u_{r,zz}+\frac{C}{2r}u_{\theta,\theta r}-\frac{1}{r^2}\left[C\left(1-\nu\right)+C'\right]u_{\theta,\theta}=\rho\left(1-\mu\nabla^2\right)\frac{\partial^2 u_r}{\partial t^2}\end{aligned} \tag{6-1}$$

$$\begin{aligned} &C'u_{z,rr}+\frac{C'}{r}u_{z,r}+C\left(1-\nu\right)u_{z,zz}+\frac{C'}{r^2}u_{z,\theta\theta}+\frac{C}{2}u_{r,rz}+\frac{C}{2r}u_{r,z}+\frac{C}{2r}u_{\theta,\theta z}\\ &=\rho\left(1-\mu\nabla^2\right)\frac{\partial^2 u_z}{\partial t^2}\end{aligned} \tag{6-2}$$

$$\begin{aligned} &C'u_{\theta,rr}+\frac{C'}{r}u_{\theta,r}-\frac{C'}{r^2}u_{\theta}+C'u_{\theta,zz}+\frac{C}{2r}u_{r,r\theta}+\frac{1}{r^2}\left[C\left(1-\nu\right)+C'\right]u_{r,\theta}+\frac{C}{2r}u_{z,\theta z}\\ &=\rho\left(1-\mu\nabla^2\right)\frac{\partial^2 u_\theta}{\partial t^2}\end{aligned} \tag{6-3}$$

3 EXACT SOLUTION

The following non-dimensional parameters are adopted to present a more general solution,

$$\overline{\sigma}_{ij}=\frac{\sigma_{ij}}{P},\ \Omega_{ij}=\omega_{ij}R\sqrt{\frac{\rho}{E}},\ \overline{z}=\frac{z}{L},\ \overline{r}=\frac{r}{R},\ \overline{\mu}=\frac{\mu}{L^2},\ \overline{u}=\frac{u}{h} \tag{7}$$

R is the inner radius and P is the external pressure. The exact solution to SWCNTs with simply supported edges should satisfy the following edges conditions:

$$u_r=u_\theta=\sigma_z=0 \quad at\ \ z=0,L \tag{8}$$

The following solutions satisfy the simply supported boundary conditions,

$$\begin{aligned} \overline{u}_r\left(\overline{r},\theta,\overline{z}\right)&=U_r^*\sin\left(\overline{p}_n\overline{z}\right)\cos\left(m\theta\right)\\ \overline{u}_\theta\left(\overline{r},\theta,\overline{z}\right)&=U_\theta^*\sin\left(\overline{p}_n\overline{z}\right)\sin\left(m\theta\right)\\ \overline{u}_z\left(\overline{r},\theta,\overline{z}\right)&=U_z^*\cos\left(\overline{p}_n\overline{z}\right)\cos\left(m\theta\right)\\ \overline{\sigma}_r\left(\overline{r},\theta,\overline{z}\right)&=\sigma_r^*\sin\left(\overline{p}_n\overline{z}\right)\cos\left(m\theta\right)\\ \overline{\tau}_{r\theta}\left(\overline{r},\theta,\overline{z}\right)&=\tau_{r\theta}^*\sin\left(\overline{p}_n\overline{z}\right)\cos\left(m\theta\right)\\ \overline{\tau}_{rz}\left(\overline{r},\theta,\overline{z}\right)&=\tau_{rz}^*\cos\left(\overline{p}_n\overline{z}\right)\cos\left(m\theta\right)\end{aligned}$$

$$\begin{aligned}\overline{\sigma}_z\left(\overline{r},\theta,\overline{z}\right) &= \sigma_z^* \sin\left(\overline{p}_n\overline{z}\right)\cos\left(m\theta\right)\\ \overline{\tau}_{z\theta}\left(\overline{r},\theta,\overline{z}\right) &= \tau_{z\theta}^* \cos\left(\overline{p}_n\overline{z}\right)\sin\left(m\theta\right)\\ \overline{\sigma}_\theta\left(\overline{r},\theta,\overline{z}\right) &= \sigma_\theta^* \sin\left(\overline{p}_n\overline{z}\right)\cos\left(m\theta\right)\end{aligned} \tag{9}$$

where $\overline{p}_n = n\pi$ and $U_r^*, U_\theta^*, U_z^*, \sigma_r^*, \sigma_z^*, \sigma_\theta^*, \tau_{rz}^*, \tau_{r\theta}^*, \tau_{z\theta}^*$ are functions of r. Substitution of relations (9) into the Eqs. (6-1) - (6-3) yields the following state equations

$$\frac{d}{d\overline{r}}\left\{\delta\right\} = G\left\{\delta\right\} \tag{10}$$

where $\left\{\delta\right\} = \left\{U_r^* \quad U_\theta^* \quad U_z^* \quad U_{r,\bar{r}}^* \quad U_{\theta,\bar{r}}^* \quad U_{z,\bar{r}}^*\right\}^T$ and G is the coefficient matrix (see appendix).
The general solution to Eq. (11) explicitly expressed as

$$\left\{\delta\left(\overline{r}\right)\right\} = \exp\left[\int_1^{\overline{r}} G d\overline{r}\right]\left\{\delta_0\right\} \tag{11}$$

where $\left\{\delta_0\right\} = \left\{\delta(\overline{r})\right\}\big|_{\overline{r}=1}$.

3.1 Free Vibration

In the free vibration analysis, the inner surface is traction free and the outer surface is surrounded by elastic medium. The elastic foundation is assumed to have both shear and transverse flexibilities. So that, the boundary conditions are as follow;

$$\begin{aligned}&\sigma_r = \tau_{r\theta} = \tau_{rz} = 0 && at \;\; r = R_i\\ &\sigma_r = -k_r u_r + k_g \nabla^2 u_r, \tau_{r\theta} = \tau_{rz} = 0 && at \;\; r = R_o\end{aligned} \tag{12}$$

where k_r and k_g are transverse and shear elastic foundation, respectively. By using Eq. (11), a relationship between the state vectors on the outer and inner surfaces of the shell is established as

$$\left\{\delta_h\right\} = \left[S\right]\left\{\delta_0\right\} \tag{13}$$

where $\left\{\delta_h\right\} = \left\{\delta\left(\overline{r}\right)\right\}\Big|_{\overline{r}_o}$ and $\left[S\right] = \exp(\int_1^{\overline{r}_o} G d\overline{r})$ From Eqs. (5-1), (5-4) and (5-5) the surface boundary conditions Eqs. (12) can be written in terms of displacements and their derivatives;

$$\begin{bmatrix}\left[A\right]_{3\times 6}\\ \left[B\right]_{3\times 6}\times\left[S\right]_{6\times 6}\end{bmatrix}\left\{\delta_0\right\} = \left\{0\right\}_{6\times 1} \tag{14}$$

where [A] and [B] are constant coefficient matrixes, respectively (appendix). To obtain nontrivial solution for Eq. (14), the determinant of matrix coefficient in the left hand should be set to zero. By solving the obtained equation, natural frequency of CNTs is obtained.

3.2 Bending Analysis

In the bending analysis, it is assumed that the outer surface is exposed to uniform pressure. The boundary conditions in the inner and outer surface for bending analysis are considered as below;

$$\begin{aligned} &\sigma_r = \tau_{r\theta} = \tau_{rz} = 0 && at \;\; r = R_i \\ &\sigma_r = -P - k_r u_r + k_g \nabla^2 u_r \,, \tau_{r\theta} = \tau_{rz} = 0 && at \;\; r = R_o \end{aligned} \tag{15}$$

From Eqs. (5-1), (5-4) and (5-5) the surface boundary conditions, Eqs. (15), are changed to the displacement components and can rewritten as below;

$$\begin{bmatrix} [A]_{3\times 6} \\ [B]_{3\times 6} \times [S]_{6\times 6} \end{bmatrix} \{\delta_0\} = \{D\}_{6\times 1} \tag{16}$$

By solving Eq. (16), the displacements and their derivatives, δ_0, at the inner surface are obtained. The other state variables can be obtained by using Eq. (11). Unlike the local theory, the stress components cannot calculate directly from displacement components. On the other hand for obtaining stress component, one should solve the nonlocal differential equations of stress-displacement relations (Eqs. (5)). Here, the state space technique is used again to reformulating the stress components. By applying state space technique to the stress-displacement relations, Eq. (5), and using the obtained displacement components, the through the thickness stress distribution is derived as follow

$$\frac{d}{d\bar{r}} \begin{Bmatrix} \sigma^*_{ij} \\ \sigma^*_{ij,\bar{r}} \end{Bmatrix} = [H] \begin{Bmatrix} \sigma^*_{ij} \\ \sigma^*_{ij,\bar{r}} \end{Bmatrix} - \frac{R^2}{\mu} \begin{Bmatrix} 0 \\ f\left(u^*_i\right) \end{Bmatrix}, \; H = \begin{bmatrix} 0 & 1 \\ \dfrac{R^2}{\mu}\left(1 + \mu\, p_n^2 + \mu\left(\dfrac{m}{R\bar{r}}\right)^2\right) & -\dfrac{1}{\bar{r}} \end{bmatrix} \tag{17}$$

where H and $f(u_i^*)$ are coefficient matrix and scalar, respectively (see appendix). Eq. (17) can be solved by using a similar manner like Eq. (10). From Eq. (16) as well as surface boundary conditions, Eq. (15), the transverse stresses can be derived and then from Eq. (2) the in-plane stress is determined.

4 NUMERICAL RESULTS AND DISCUSSION

In this section, the following material and geometrical properties are assumed for SWCNTs: Young's modulus *E=1.06 Tpa*, inner radius *R=2.32 nm* and Poisson's ratio *ν=0.3* [28] Alibeigloo and Shaban (2013) . For comparison study, at first, the results of free vibration for thin and thick cylindrical shell (μ=0) with finite length are obtained and compared respectively with the results of Murmu and Pradhan (2009) according to Table 1 and Qatu (2004) as mention in Table 2. Excellent agreement between results can be observed for thin and thick cylinders. Secondly, validation of the bending analysis is carried out by using commercial finite element code ABAQUS. Table 3 shows the numerical results of radial deflection for isotropic cylinder subjected to uniform internal pressure (P_{in} = *80 Mpa*). As the table shows, the obtained results are in good agreement with numerical analysis.

n	M	Results	Qatu (2004)
1	**0**	0.97087	0.96852
	1	0.59721	0.59729
	2	0.34025	0.34038
	3	0.20145	0.20149
	4	0.12886	0.12908
	5	0.09105	0.09104
2	**0**	0.99351	0.99501
	1	0.88357	0.88441
	2	0.68072	0.68107
	3	0.50059	0.50153
	4	0.36918	0.36908
	5	0.27671	0.27711

Table 1: Comparisons of natural frequency for thin cylindrical shell

$$\Omega_{nm}\,(\,\nu = 0.285, \frac{h}{R} = 0.0034, \frac{L}{R} = 2\,)$$

h/R	m	Results	SOLDATOS and P. (1990)
0.1	**1**	0.913	0.932
	2	0.762	0.774
	3	0.699	0.710
0.2	**1**	0.993	1.043
	2	0.936	0.966
	3	0.999	1.051
0.3	**1**	1.112	1.173
	2	1.116	1.161
	3	1.245	1.340

Table 2: Comparisons of natural frequency for thick cylindrical shell $\Omega_{nm}\,(\,\frac{L}{R} = 1, n = 1\,)$

$\frac{h}{R}$	$\frac{L}{R}$	$u_r\left(10^{-5}m\right)$	**Abaqus**
0.3	5	6.6931	6.599
	15	6.7181	6.563
	25	6.7181	6.557
0.5	5	4.7177	4.604
	15	4.6409	4.639
	25	4.6409	4.636
1	5	3.31	3.21
	15	3.1488	3.136
	25	3.1491	3.134

Table 3 Comparison of radial deflection for isotropic cylinder
($E = 200\ G\ pa$, $R_i = 40\ mm$, $\nu = 0.3$)

After comparision with macro structures, furthere comparision is provided by considering single wall armchair (15, 15) and zigzag (26, 0) nano tubes. An accurate discreate nano-scale finite element (FE) model was studied in work done by Seifoori and Liaghat (2013) to obtain mechanical and geomertical properties of mensioned SWCNTs, and compared with other investigations. The mechanical and geomertical properties of (15, 15) and (26, 0) SWCNTs as a thick cylindrical shell are as follow (Seifoori and Liaghat (2013)): Diameter *2.04 nm*, Young's modulus E=*1.04 GPa*, wall thickness t=*0.34 nm*, length L=*20.732 nm* and the mass density ρ=*935 kg/m*^{3}. The 3D 8-node brick elements (C3D8R) are used to generate the FE model in ABAQUS. The radial deflection and first frequency of SWCNTs computed throught state-space approach compared with those obtained by FE method. It is clear that the results agree very well with FE method and the difference is not more than 5%.

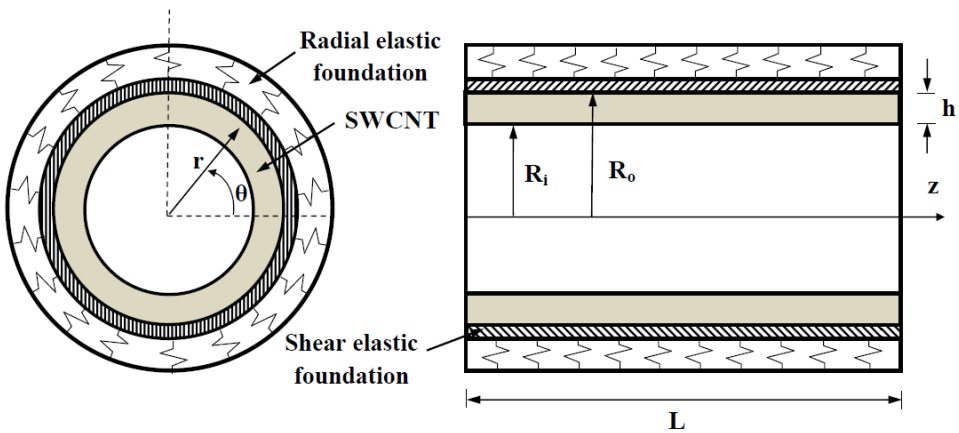

Figure 1 Single-walled carbon nanotube surrounded by polymer matrix

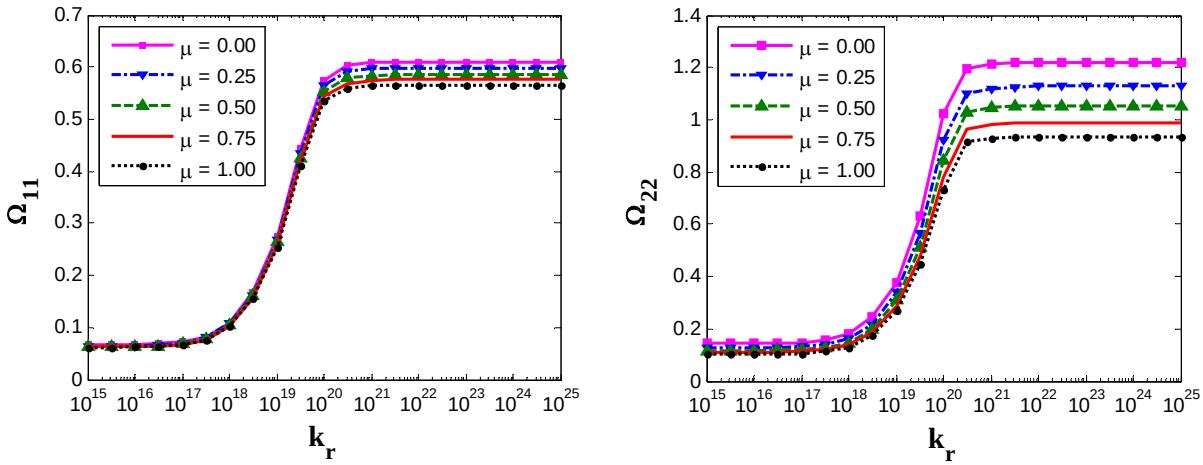

Figure 2: Variation of non-dimensional natural frequencies Ω_{nm} vs. radial elastic foundation stiffness for different values of nonlocal parameters $k_g = 0, \frac{L}{R} = 10, \frac{h}{R} = 0.14$

Here, numerical results for free vibration and bending behavior of SWCNT are carried out and presented in Tables 4-5 and Figs. 2-9. In Table 4, the first four non-dimensional natural frequencies are presented for different radial and shear stiffness values. According to this table, one can see that Ω_{nm} is very sensitive to elastic stiffness. For instance, the non-dimensional frequency of SWCNTs in the absence of elastic medium is 63% smaller than embedded SWCNTs with $k_r=10^{18}$. Fig. 2 shows the effect of variation of radial elastic foundation stiffness on the nondimensional frequency parameters Ω_{nn} for different values of nonlocal parameter μ. It can be seen that in the absence of k_g, when the k_r is less than 10^{17}, the Ω_{nn} is independent of k_r. It is also observed that fundamental frequencies of SWCNT increase abruptly with increasing k_r from about 10^{17} to 10^{21}. For k_r larger than 10^{21} the Ω_{nn} remains constant when k_r varies. From this figure it is obvious that increasing the nonlocal parameter, μ, causes the natural frequencies to decrease. Such variations are more considerable for higher modes. In a similar manner, the influence of variation of nondimensional frequency parameter Ω_{nn} versus shear elastic foundation stiffness, k_g is shown in Fig. 3. Similar behavior can be observed due to variation of k_g. According to Fig. 3, the Ω_{nn} is not affected by shear elastic foundation stiffness variation when $k_g<1$ or $k_g>10^4$. From this figure, it is clear that increasing the nonlocal parameter for small values of the k_r does not affect the nondimensional frequency parameter Ω_{nn} of SWCNTs, while, for higher values of k_r, the frequency curves get separated as μ increases.

Number of solid elements			**u_r (nm)**		**ω_{11} (THz)**	
Along the circumference	Along the axis	Along the thickness	analytical	Abaqus	analytical	Abaqus
58	163	3	3.26	3.38	44.37	46.7

Table 4: Comparison of radial deflection and first frequency of armchair (15, 15) and zigzag (26, 0) obtained from analytical solution with 3D finite element results

k_r	k_g	Ω_{11}	Ω_{12}	Ω_{21}	Ω_{22}
0	0	0.064	0.085	0.190	0.109
	2	0.078	0.123	0.193	0.141
	4	0.088	0.155	0.197	0.169
$\mathbf{10^{18}}$	0	0.102	0.120	0.204	0.137
	2	0.113	0.151	0.211	0.165
	4	0.120	0.180	0.214	0.186
$\mathbf{10^{20}}$	0	0.543	0.805	0.582	0.781
	2	0.547	0.809	0.582	0.784
	4	0.547	0.812	0.582	0.788
$\mathbf{10^{22}}$	0	0.578	0.960	0.652	0.987
	2	0.578	0.960	0.652	0.987
	4	0.578	0.960	0.652	0.987

Table 5: The first four non-dimensional natural frequencies Ω_{nm} for different radial and shear stiffness values $\frac{L}{R}=10, \frac{h}{R}=0.14, \mu=0.75\,nm^2$

Figs. 4 show variation of non-dimensional frequencies versus radial elastic foundation stiffness for different shear stiffness coefficients. It is observed that non-dimensional frequency increases rapidly with increasing k_r or k_g, as expected. Such increments are more considerable for small values of k_g and for higher values of that parameter, increasing the shear elastic foundation will cause the natural frequencies of SWCNT to increase very slightly so that for $k_g \geq 10^4$, the frequency remains constant. Considering the prior discussions, it is clear that shear elastic stiffness is dominant compared with radial stiffness and more affects the Ω_{nm}.

Figs. 5a-b show the effect of radial elastic foundation stiffness on the non-dimensional radial stress for different values of nonlocal parameter μ. Similar to Fig. 2, it can be seen that increase of k_r from about 10^{17} to 10^{21}, cause dramatic increase in the $\bar{\sigma}_r$. It can be seen that for the same values of geometrical parameters, the nonlocal parameter has more effect in the higher values of k_r on the frequency parameter. Furthermore, the discrepancy between different values of non-local parameters increases as the h/R ratio increases. Figs. 6 show variation of non-dimensional radial deflection $\bar{u}_r$ and stress $\bar{\sigma}_r$ versus radial elastic foundation stiffness for different values of shear elastic foundation stiffness. It is observed that $\bar{u}_r$ and $\bar{\sigma}_r$ decreases abruptly with increasing k_r or k_g. For $k_g > 10^{21}$ the $\bar{u}_r$ becomes zero, implying that at this elastic foundation coefficient, the foundation behaves rigidly. Table 5 shows the effect of thickness (h/R) on the non-dimensional displacement and radial stress. According to Table 6 and as expected, increase the thickness-to-radius ratio, cause the non-dimensional radial deflection and stress of the SWCNTs to decreases. Figs. 7a-b shows the effect of dimensionless ratio L/R on the first and second non-dimensional frequency. As shown in Figs. 7, when the length-to-radius ratio increased, the dimensionless frequency, decreased. Fig. 8 presents the ratio of nonlocal stress to local stress at the mid surface of SWCNT for various nonlocal parameter μ. From this figure one can conclude that for small length-to-radius ratio, the local continuum model tends to overestimate the stress. Also it can be

seen that by decreasing the L/R ratio, the effect of nonlocal parameter decreased and in this work this effect is negligible.

In Fig. 9, variation of radial stress at the mid radius along the axis of CNT subjected to uniform radial pressure with respect to different values of nonlocal parameter is presented. From Fig. 9 it can be concluded that by increasing the nonlocal parameter, the radial stress decrease.

k_r	k_g	$\frac{h}{R}=0.05$		$\frac{h}{R}=0.14$		$\frac{h}{R}=0.3$	
		$\frac{u_r}{h}(nm)$	$\frac{\sigma_r}{P}$	$\frac{u_r}{h}(nm)$	$\frac{\sigma_r}{P}$	$\frac{u_r}{h}(nm)$	$\frac{\sigma_r}{P}$
0	0	-.4031	-.4429	-.0528	-.4966	-.0149	-.5265
	10^{16}	-.4031	-.4429	-.0528	-.4966	-.0149	-.5265
	10^{18}	-.3272	-.4431	-.0506	-.4962	-.0147	-.5259
$\mathbf{10^{18}}$	0	-.3852	-.4428	-.0519	-.4964	-.0148	-.5260
	10^{16}	-.3852	-.4430	-.0519	-.4964	-.0148	-.5260
	10^{18}	-.3165	-.4431	-.0498	-.4960	-.0146	-.5255
$\mathbf{10^{20}}$	0	-.0712	-.4420	-.0191	-.4902	-.0074	-.5043
	10^{16}	-.0712	-.4422	-.0191	-.4902	-.0074	-.5043
	10^{18}	-.0710	-.4425	-.0190	-.4902	-.0074	-.5043

Table 6: Non-dimensional radial deflection and radial stress for different radial and shear stiffness values $\frac{L}{R}=10, \mu=0.75\,nm^2$ and various $\frac{h}{R}$ ratios

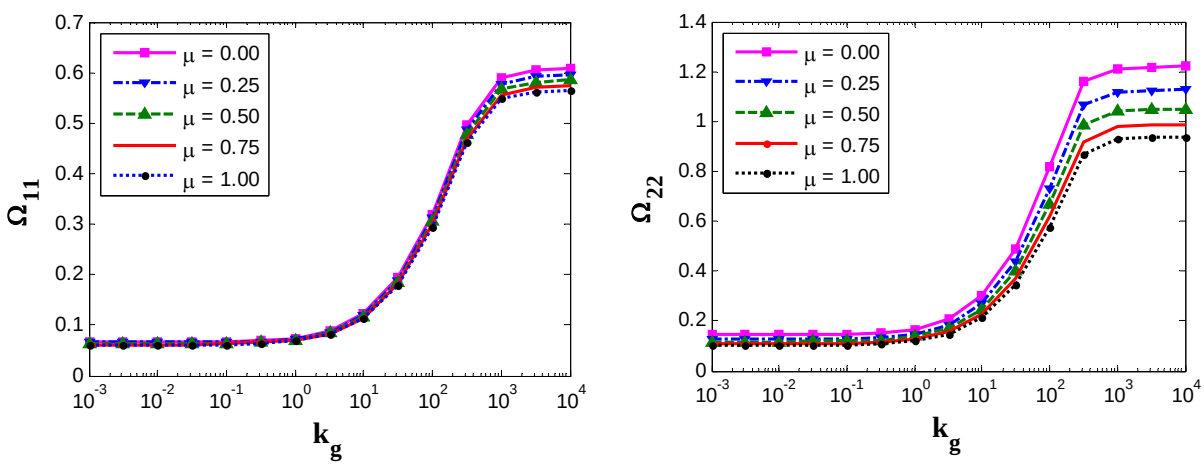

Figure 3: Variation of non-dimensional natural frequencies Ω_{nm} vs. shear elastic foundation stiffness for different values of nonlocal parameters $k_r=0, \frac{L}{R}=10, \frac{h}{R}=0.14$

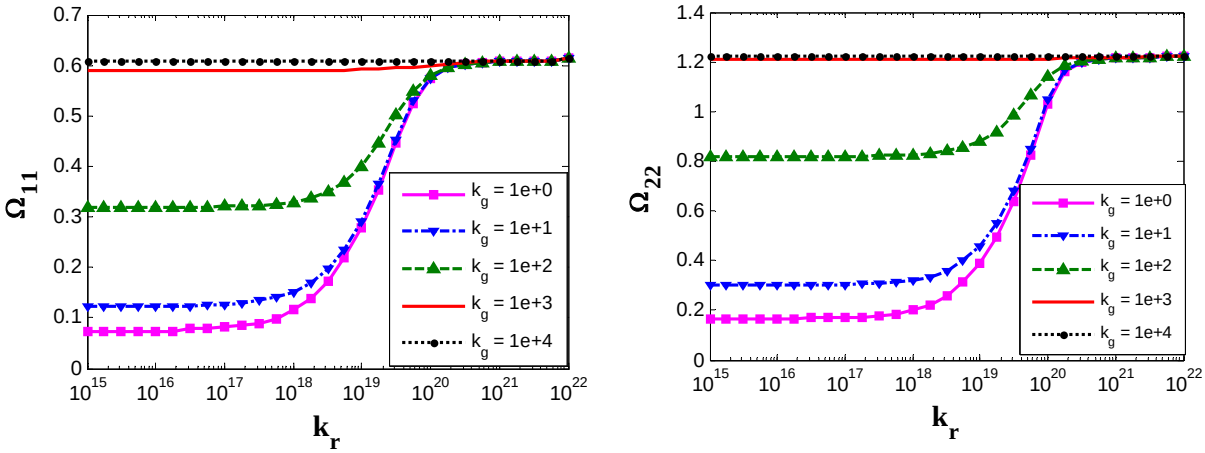

Figure 4: Variation of non-dimensional natural frequencies vs. radial elastic foundation stiffness for different values of shear elastic foundation stiffness $\mu = 0.nm^2$ $\frac{L}{R} = 10$, $\frac{h}{R} = 0.14$

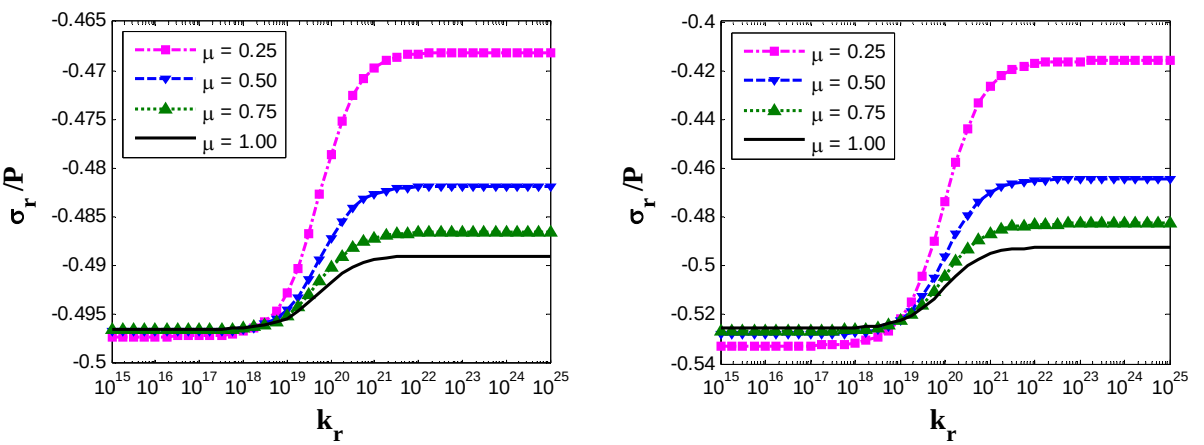

(a) **(b)**

Figure 5: Variation of non-dimensional radial stress vs. radial elastic foundation stiffness for different values of nonlocal parameters, $k_g = 0, \frac{L}{R} = 10, \mu = 0.75nm^2$ *a)* $\frac{h}{R} = 0.14$ *b)* $\frac{h}{R} = 0.3$

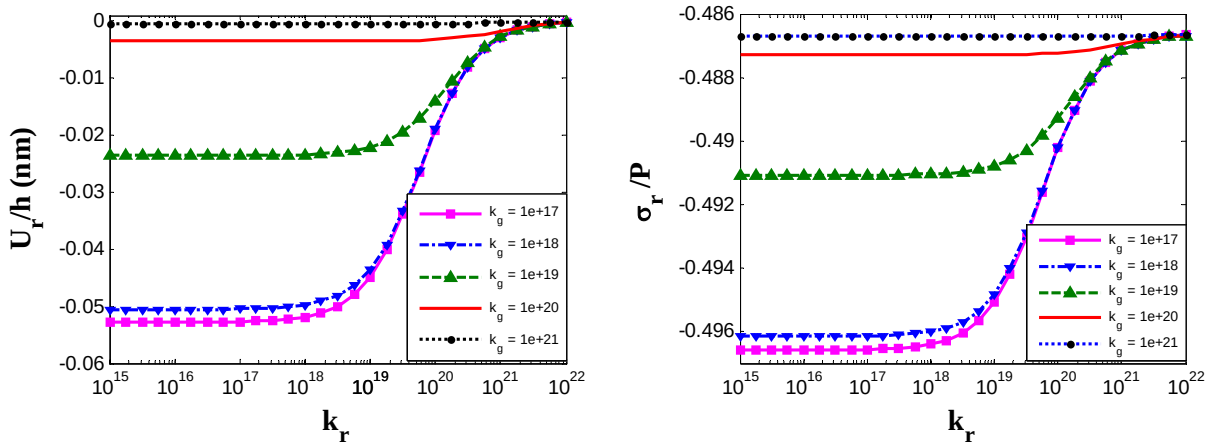

Figure 6: Variation of non-dimensional radial deflection $\overline{u}_r$ and $\overline{\sigma}_r$ vs. radial elastic foundation stiffness for different values of shear elastic foundation stiffness $\frac{h}{R} = 0.14, \frac{L}{R} = 10, \mu = 0.75\, nm^2$

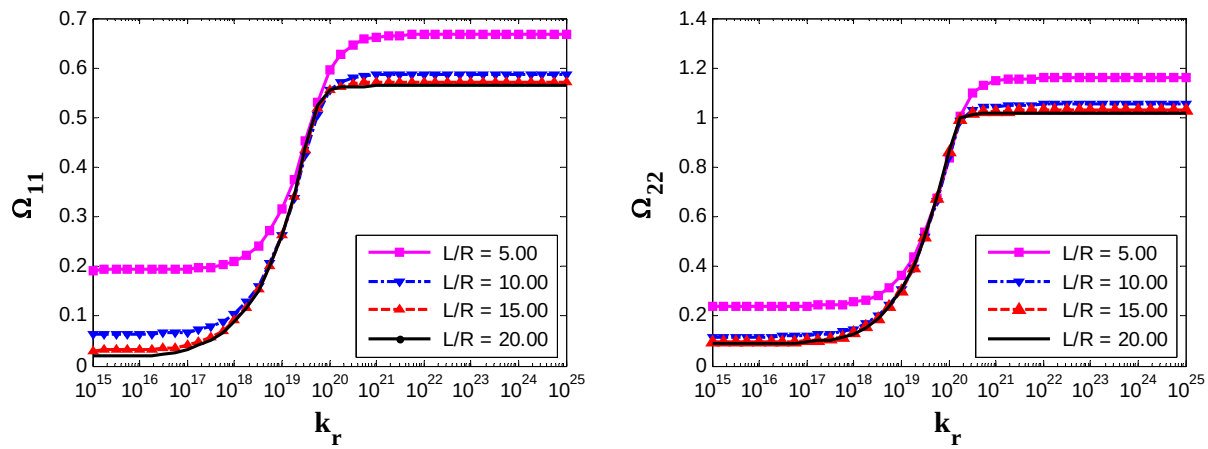

Figure 7: Variation of non-dimensional natural frequencies vs. radial elastic foundation stiffness for different values of length $k_g = 0, \frac{h}{R} = 0.14, \mu = 0.5\, nm^2$

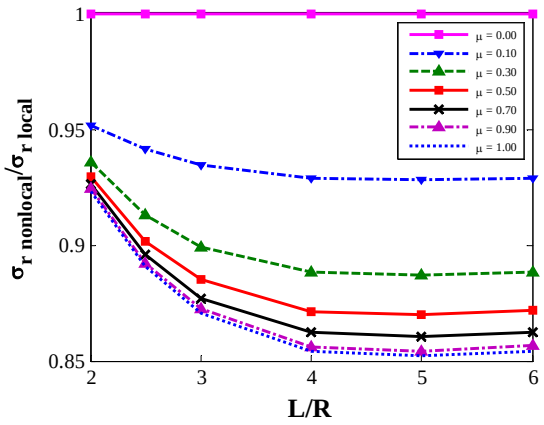

Figure 8 Effect of nonlocal parameter μ in the radial stressat $\overline{z} = \overline{r} = 0.5, \frac{h}{R} = 0.6, k_r = k_g = 0$

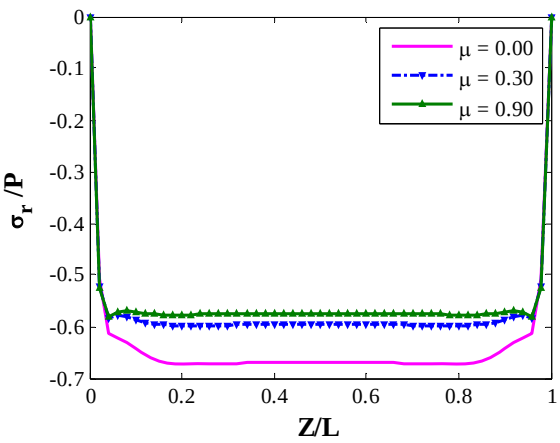

Figure 9 Axial distrubution of radial stress and displacement with various nonlocal parameter μ at

$$\overline{r} = 0.5, \frac{h}{R} = 0.6, \frac{L}{R} = 10, k_r = k_g = 0$$

5 CONCLUSION

An accurate solution procedure based on the three-dimensional theory of elasticity for the bending and free vibration analysis of embedded SWCNTs is presented. It is assumed that SWCNT is surrounded by elastic medium with both radial and shear stiffness. The nonlocal elasticity is adopted to constitutive relations to investigate the size effect of CNTs. Using the series expansion of stress and displacement components through the axial and tangential directions, equations of motion and the related boundary conditions were developed. After that, the state-space method was used to solve the resulting equations of motion along the thickness direction. The obtained solutions provide a better representation of the bending and vibration behavior of short nanotubes where the effects of small scale and elastic medium are significant. It is concluded that small scale parameter has a substantial effect on the natural frequency and radial stress and dis-

placement of SWCNTs and neglecting this effect leads to significant errors. In addition, it is presented that higher modes of natural frequencies are more sensitive to the small length scale. This study shows that the static and vibrational behaviors of SWCNTs are strongly affected by elastic medium. It is observed that radial and shear stiffness in a special interval become more pronounced, and cause the natural frequency and radial stress and displacement to be increased rapidly. Also, the effect of length to radius ratio is examined. The presented nonlocal shell model is useful for study and design of embedded nanotube-based devices.

References

Alibeigloo, A., 2011. Free vibration analysis of nano-plate using three-dimensional theory of elasticity. *Acta Mechanica*, 222(1-2), pp.149–159.

Alibeigloo, A., 2012. Three-dimensional free vibration analysis of multi-layered graphene sheets embedded in elastic matrix. *Journal of Vibration and Control*, 19(16), pp.2357–2371.

Alibeigloo, A. & Pasha Zanoosi, A., 2013. Static analysis of rectangular nano-plate using three-dimensional theory of elasticity. *Applied Mathematical Modelling*, 37(10-11), pp.7016–7026.

Alibeigloo, A. & Shaban, M., 2013. Free vibration analysis of carbon nanotubes by using three-dimensional theory of elasticity. *Acta Mechanica*, 224(7), pp.1415–1427.

Ansari, R., Hemmatnezhad, M. & Rezapour, J., 2011. The thermal effect on nonlinear oscillations of carbon nanotubes with arbitrary boundary conditions. *Current Applied Physics*, 11(3), pp.692–697.

Ansari, R., Rouhi, H. & Sahmani, S., 2011. Calibration of the analytical nonlocal shell model for vibrations of double-walled carbon nanotubes with arbitrary boundary conditions using molecular dynamics. *International Journal of Mechanical Sciences*, 53(9), pp.786–792.

Ansari, R. & Sahmani, S., 2011. Bending behavior and buckling of nanobeams including surface stress effects corresponding to different beam theories. *International Journal of Engineering Science*, 49(11), pp.1244–1255.

Ansari, R., Sahmani, S. & Rouhi, H., 2011. Rayleigh–Ritz axial buckling analysis of single-walled carbon nanotubes with different boundary conditions. *Physics Letters A*, 375(9), pp.1255–1263.

Arash, B. & Ansari, R., 2010. Evaluation of nonlocal parameter in the vibrations of single-walled carbon nanotubes with initial strain. *Physica E: Low-dimensional Systems and Nanostructures*, 42(8), pp.2058–2064.

Aydogdu, M., 2012. Axial vibration analysis of nanorods (carbon nanotubes) embedded in an elastic medium using nonlocal elasticity. *Mechanics Research Communications*, 43, pp.34–40.

Aydogdu, M. & Filiz, S., 2011. Modeling carbon nanotube-based mass sensors using axial vibration and nonlocal elasticity. *Physica E: Low-dimensional Systems and Nanostructures*, 43(6), pp.1229–1234.

Eltaher, M. a., Emam, S. a. & Mahmoud, F.F., 2012. Free vibration analysis of functionally graded size-dependent nanobeams. *Applied Mathematics and Computation*, 218(14), pp.7406–7420.

Eringen, A.C., 2002. *Nonlocal Continuum Field Theories*, Springer.

Gibson, R.F., Ayorinde, E.O. & Wen, Y.-F., 2007. Vibrations of carbon nanotubes and their composites: A review. *Composites Science and Technology*, 67(1), pp.1–28.

Hao, M.J., Guo, X.M. & Wang, Q., 2010. Small-scale effect on torsional buckling of multi-walled carbon nanotubes. *European Journal of Mechanics - A/Solids*, 29(1), pp.49–55.

He, X.Q., Kitipornchai, S. & Liew, K.M., 2005. Buckling analysis of multi-walled carbon nanotubes: a continuum model accounting for van der Waals interaction. *Journal of the Mechanics and Physics of Solids*, 53(2), pp.303–326.

Hu, Z.L., Guo, X.M. & Ru, C.Q., 2008. Enhanced critical pressure for buckling of carbon nanotubes due to an inserted linear carbon chain. *Nanotechnology*, 19(30), p.305703.

Hu, Z.L., Guo, X.M. & Ru, C.Q., 2007. The effects of an inserted linear carbon chain on the vibration of a carbon nanotube. *Nanotechnology*, 18(48), p.485712.

Khademolhosseini, F., Rajapakse, R.K.N.D. & Nojeh, a., 2010. Torsional buckling of carbon nanotubes based on nonlocal elasticity shell models. *Computational Materials Science*, 48(4), pp.736–742.

Murmu, T., Adhikari, S. & Wang, C.Y., 2011. Torsional vibration of carbon nanotube–buckyball systems based on nonlocal elasticity theory. *Physica E: Low-dimensional Systems and Nanostructures*, 43(6), pp.1276–1280.

Murmu, T. & Pradhan, S.C., 2009. Buckling analysis of a single-walled carbon nanotube embedded in an elastic medium based on nonlocal elasticity and Timoshenko beam theory and using DQM. *Physica E: Low-dimensional Systems and Nanostructures*, 41(7), pp.1232–1239.

Qatu, M.S., 2004. *Vibration Of Laminated Shells And Plates* 1st ed., Elsevier Ltd.

Reddy, J.N., 2007. Nonlocal theories for bending, buckling and vibration of beams. *International Journal of Engineering Science*, 45(2-8), pp.288–307.

Seifoori, S. & Liaghat, G.H., 2013. Low velocity impact of a nanoparticle on nanobeams by using a nonlocal elasticity model and explicit finite element modeling. *International Journal of Mechanical Sciences*, 69, pp.85–93.

Shen, Z.-B. *et al.*, 2012. Nonlocal Timoshenko beam theory for vibration of carbon nanotube-based biosensor. *Physica E: Low-dimensional Systems and Nanostructures*, 44(7-8), pp.1169–1175.

Soldatos, K.P. & P., H. V., 1990. Three-dimensional Problem Solution Shells of the Free Vibration Isotropic of Homogeneous Cylindrical. *Journal of Sound and Vibration*, 137(3), pp.369–384.

Sun, C.T. & Zhang, H., 2003. Size-dependent elastic moduli of platelike nanomaterials. *Journal of Applied Physics*, 93(2), p.1212.

Thai, H.-T., 2012. A nonlocal beam theory for bending, buckling, and vibration of nanobeams. *International Journal of Engineering Science*, 52, pp.56–64.

Wang, C.M. *et al.*, 2006. Buckling analysis of micro-and nano-rods/tubes based on nonlocal Timoshenko beam theory. *Journal of Physics D: Applied Physics*, 39(17), p.3904.

Wang, C.Y. *et al.*, 2012. Circumferential nonlocal effect on vibrating nanotubules. *International Journal of Mechanical Sciences*, 58(1), pp.86–90.

Wang, Q. & Liew, K.M., 2007. Application of nonlocal continuum mechanics to static analysis of micro- and nano-structures. *Physics Letters A*, 363(3), pp.236–242.

Yan, Y., Wang, W.Q. & Zhang, L.X., 2010. Nonlocal effect on axially compressed buckling of triple-walled carbon nanotubes under temperature field. *Applied Mathematical Modelling*, 34(11), pp.3422–3429.

Yoon, J., 2003. Vibration of an embedded multiwall carbon nanotube. *Composites Science and Technology*, 63(11), pp.1533–1542.

Appendix:

$$G=\begin{bmatrix} 0 & 0 & 0 & 1 & 0 & 0 \\ 0 & 0 & 0 & 0 & 1 & 0 \\ 0 & 0 & 0 & 0 & 0 & 1 \\ G_{41} & G_{42} & 0 & G_{44} & G_{45} & G_{46} \\ G_{51} & G_{52} & G_{53} & G_{54} & G_{55} & 0 \\ G_{61} & G_{62} & G_{63} & G_{64} & 0 & G_{66} \end{bmatrix}$$

where:

$$G_{44}=G_{55}=G_{66}=-\frac{1}{\overline{r}} \qquad G_{41}=\frac{1}{\overline{r}^2}+\frac{C'}{C\left(1-\nu\right)}\left\{\frac{m^2}{\overline{r}^2}+\overline{p}_n^2\frac{R^2}{L^2}\right\}$$

$$G_{42}=\frac{m}{\overline{r}^2}\left\{1+\frac{C'}{C\left(1-\nu\right)}\right\} \qquad G_{45}=-\frac{1}{\left(1-\nu\right)}\frac{m}{2\overline{r}}$$

$$G_{46}=\frac{1}{\left(1-\nu\right)}\frac{R}{2L}\overline{p}_n^2 \qquad G_{51}=\frac{m}{\overline{r}^2}\left\{\frac{C\left(1-\nu\right)}{C'}+1\right\}$$

$$G_{52}=\frac{1}{\overline{r}^2}\left\{\frac{m^2C\left(1-\nu\right)+1}{C'}\right\}+\overline{p}_n^2\frac{R^2}{L^2} \qquad G_{53}=-\frac{C}{C'}\left\{\frac{R}{L}\frac{m\overline{p}_n}{2\overline{r}}\right\}$$

$$G_{54}=\frac{C}{C'}\frac{m}{2\overline{r}} \qquad G_{61}=-\frac{C}{C'}\left\{\frac{\overline{p}_n}{2\overline{r}}\frac{R}{L}\right\}$$

$$G_{62}=-\frac{C}{C'}\left\{\frac{R}{L}\frac{m\overline{p}_n}{2\overline{r}}\right\} \qquad G_{63}=\frac{m^2}{\overline{r}^2}+\frac{C}{C'}\overline{p}_n^2\left(1-\nu\right)\frac{R^2}{L^2}$$

$$G_{64}=-\frac{C}{C'}\left\{\frac{\overline{p}_n}{2}\frac{R^2}{L^2}\right\}$$

$$\left[A\right]_{3\times6}=\frac{h}{R}\begin{bmatrix} \overline{C}\nu & \overline{C}\nu m & -\overline{C}\nu\dfrac{R}{L}\overline{p}_n & \overline{C}\left(1-\nu\right) & 0 & 0 \\ \overline{C}'\nu\dfrac{R}{L}\overline{p}_n & 0 & 0 & 0 & 0 & \overline{C}' \\ -\overline{C}'m & -\overline{C}' & 0 & 0 & \overline{C}' & 0 \end{bmatrix}$$

$$\left[B\right]_{3\times 6}=\frac{h}{R}\begin{bmatrix}\dfrac{\bar{C}\nu R}{R_o}+\dfrac{R}{E}\left(k_r+k_g\left(\bar{p}_n{}^2+\left(\dfrac{m}{R_o}\right)^2\right)\right) & \bar{C}\nu m\dfrac{R}{R_o} & -\bar{C}\nu\dfrac{R}{L}\bar{p}_n & \bar{C}\left(1-\nu\right) & 0 & 0\\ \bar{C}'\nu\dfrac{R}{L}\bar{p}_n & 0 & 0 & 0 & 0 & \bar{C}'\\ -\bar{C}'m\dfrac{R}{R_o} & -\bar{C}'\dfrac{R}{R_o} & 0 & 0 & \bar{C}' & 0\end{bmatrix}$$

$$\left\{D\right\}=\begin{Bmatrix}0\\0\\0\\Q\left\{P\right\}\\0\\0\end{Bmatrix},\quad Q=\left[1+\bar{\mu}\,\bar{p}_n^2+\frac{L^2}{R_o{}^2}m^2-\bar{\mu}\frac{L^2}{R^2}\left(\frac{\partial^2}{\partial\bar{r}^2}+\frac{R}{R_o}\frac{\partial}{\partial\bar{r}}\right)\right]$$

$$H=\begin{bmatrix}0 & 1\\ \dfrac{R^2}{\mu}\left\{1+\mu\,p_n{}^2+\mu\left(\dfrac{m}{R\bar{r}}\right)^2\right\} & -\dfrac{1}{\bar{r}}\end{bmatrix}$$

$$f(\sigma_r^*)=C\left[\frac{1-\nu}{R}U^*_{r,\bar{r}}+\frac{\nu}{R}\frac{1}{\bar{r}}\left(mU_\theta^*+U_r^*\right)-\nu\,p_nU_z^*\right]$$

$$f(\sigma_\theta^*)=C\left[\frac{\nu}{R}U^*_{r,\bar{r}}+\frac{1-\nu}{R}\frac{1}{\bar{r}}\left(mU_\theta^*+U_r^*\right)-\nu\,p_nU_z^*\right]$$

$$f(\sigma_z^*)=C\left[\frac{\nu}{R}U^*_{r,\bar{r}}+\frac{\nu}{R}\frac{1}{\bar{r}}\left(mU_\theta^*+U_r^*\right)-\left(1-\nu\right)p_nU_z^*\right]$$

$$f(\tau_{rz}^*)=C'\left(\frac{1}{R}U^*_{z,\bar{r}}+p_n\,U_r^*\right)$$

$$f(\tau_{r\theta}^*)=C'\left(-\frac{m}{R}\frac{1}{\bar{r}}U_r^*+\frac{1}{R}U^*_{\theta,\bar{r}}-\frac{1}{R\bar{r}}U_\theta^*\right)$$

$$f(\tau_{z\theta}^*)=C'\left(-\frac{m}{R}\frac{1}{\bar{r}}U_z^*+p_n\,U_\theta^*\right)$$